# Assessment of Laser Transmission Mirror Materials for ITER Edge Thomson Scattering Diagnostics

Shin KAJITA[a)], Takaki HATAE and Vladimir S. VOITSENYA[1)]

*Fusion Research and Development Directorate, Japan Atomic Energy Agency, 801-1 Mukoyama, Naka, Ibaraki 311-0193, Japan*

[1)]*Institute of Plasma Physics, National Science Centre, Kharkov Institute of Science and Technology, Kharkov 61108, Ukraine*

An assessment of in-vessel metallic mirror materials for the transmission of the laser beam used in the ITER edge Thomson scattering diagnostics is reported. The transient temperature increase due to the laser pulse irradiation on the laser transmission mirror is calculated by a one-dimensional heat conduction equation. Candidate mirror materials are discussed based on a comparison between the numerical calculation and current data relevant to the laser-induced damage threshold (LIDT). Gold, silver, and copper are considered promising because of its high reflectivity. The LIDT is evaluated considering multi-pulse effects and used to determine the necessary size for the laser transmission mirror for the ITER edge Thomson scattering diagnostics.

## 1. Introduction

Plasma diagnostics in ITER requires the use of many in-vessel mirrors. And since in-vessel mirrors are exposed to neutron and gamma-ray radiations, as well as to charge-exchange particles from plasmas, metals are considered the most promising candidate materials [1]. The functions of the in-vessel mirrors can be divided into two different categories: (i) mirrors for collecting the emission from the plasma, and (ii) mirrors for the transmission of the laser beam. In selecting the material for the former, the important factor to be considered is the durability to sputtering caused by charge-exchange neutrals and the deposition of eroded material [2, 3]. As for the latter, on the other hand, the material choice requires the assessment of the laser-induced damage threshold (LIDT) [4].

One of the plasma diagnostics systems using a laser in ITER is the Thomson scattering diagnostics, which can measure the electron temperature and density. Four Thomson scattering diagnostics systems are planned to be installed in ITER, i.e., in the core, edge, X-point, and divertor regions [5]. For the edge Thomson scattering diagnostics in ITER, a 1064 nm neodymium-doped yttrium aluminum garnet (Nd:YAG) laser is currently being developed [6, 7]. The required specifications for the laser include a pulse energy of 5 J with a repetition frequency of 100 Hz and pulse width of ~10 ns.

In Ref. [1], several materials have been proposed for the in-vessel mirror for laser diagnostics and the figure-of-merit has been presented for the material choice. In the present paper, based on this proposal, the discussion focuses on the material choice for the Thomson scattering diagnostics in ITER, particularly the edge Thomson scattering system. We choose gold (Au), silver (Ag), copper (Cu), tantalum (Ta), rhodium (Rh), and molybdenum (Mo) as the candidate material. Then, based on current LIDT data and a comparison between the data and the numerically calculated temperature of the material in response to the laser irradiation, the preferred mirror material for the measurement system is discussed. Moreover, the necessary mirror size for the ITER edge Thomson scattering system is also presented.

In Sec. 2, after presenting the numerical method and necessary parameters used in the calculation, comparisons between the current LIDT data and our calculation results are made. The necessary parameters for the calculation include the thermophysical properties and optical reflectivity of the materials, which are also presented. In Sec. 3, the plausible material for the edge Thomson scattering system is discussed based on the numerical assessment; in addition, further lines of investigation that cannot be discussed in this paper are pointed out. Finally, our conclusions are listed in Sec. 4.

## 2. Current LIDT Data and Numerical Assessment

The temporal evolution of the temperature of a metal in response to a laser pulse can be determined by solving the heat conduction equation. Since the thermal diffusion

*author's e-mail: kajita@ees.nagoya-u.ac.jp*

[a)]present address: EcoTopia Science Institute, Nagoya University, Nagoya 464-8603, Japan

length is much shorter than the diameter of the laser beam, the following one-dimensional heat conduction equation is applicable:

$$c_p(T)\rho\frac{\partial T}{\partial t} = \frac{\partial}{\partial z}\left(K(T)\frac{\partial T}{\partial z}\right) + Q(z,t), \qquad (1)$$

where $c_p$ is the specific heat in $Jkg^{-1}K^{-1}$; $\rho$, the density in $kgm^{-3}$; $T$, the temperature in K; $z$, the distance from the surface in m; and $K$, the thermal conductivity in $Wm^{-1}K^{-1}$. In Eq. (1), $Q(z,t)$ is the energy absorbed by the metal in $Wm^{-3}$ and can be written as follows:

$$Q(z,t) = (1-R)I(t)\frac{\exp(-z/l_p)}{l_p}, \qquad (2)$$

where $I(t)$ is the laser power in $Wm^{-2}$; $R$, the optical reflectivity; and $l_p$, the absorption penetration depth [8]. For the calculation, the thermophysical properties and optical reflectivity of materials are necessary. Then Eq. (1) is discretized by the Crank-Nicolson scheme and the temporal evolution of the material temperature is calculated.

Figure 1 shows the temperature dependences of (a) the thermal conductivity, (b) density, and (c) specific heat for
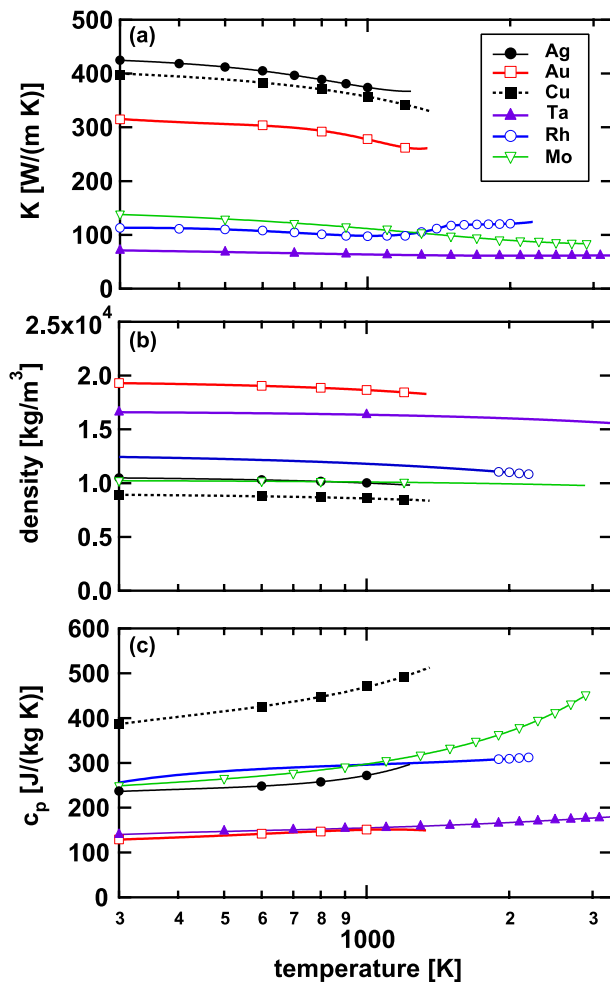


Fig. 1 Temperature dependences of (a) thermal conductivity, (b) density, and (c) specific heat for Rh, Ag, Au, Cu, Ta, and Mo.

Au, Ag, Cu, Ta, Rh, and Mo. Because of the limitation of the data, we used some functions for fitting the data and extrapolated them to the melting point. Concerning Au and Cu, the data from a thermophysical property handbook [9] were used. Ref. [9] was used for the densities of Ag, Ta, and Mo. The data in Ref. [10] were used for the specific heats and thermal conductivities of Ag, Ta, and Mo. With regard to Rh, the density in Refs. [9, 11], specific heat in Refs. [10, 11], and thermal conductivity in Refs. [12–14] were used.

Figure 2 shows the optical reflectivity as a function of the wavelength for Ag, Au, Cu, Rh, Ta, and Mo. These curves were calculated from the following relation by using the refraction index $n$ and extinction coefficient $k$ in Ref. [15]:

$$R = \frac{(n-1)^2 + k^2}{(n+1)^2 + k^2}. \qquad (3)$$

At 1064 nm, the reflectivities of Ag, Au, and Cu are much higher than 90%, while those of Rh and Ta are slightly greater than 80% and that of Mo is approximately 70%. The temperature dependence of the optical reflectivity is taken into account based on the method proposed by Ujihara [16]. It is noted that the calculation deduced significant temperature dependence, which is sometimes not consistent with the experiments referenced in [1]. Therefore, we use both the calculated and experimentally obtained reflectivity in the calculation; the differences between them are discussed later. Table 1 lists the melting points and values of coefficient $A$ for determining the temperature-dependent reflectivity $R(T)$ defined as follows:

$$R(T) = R_0(1 - AT). \qquad (4)$$

In the case of Cu, for example, it is expected from the experiments that a 1000 K increase in temperature results in a reduction of 3% in reflectivity; however, the calculations
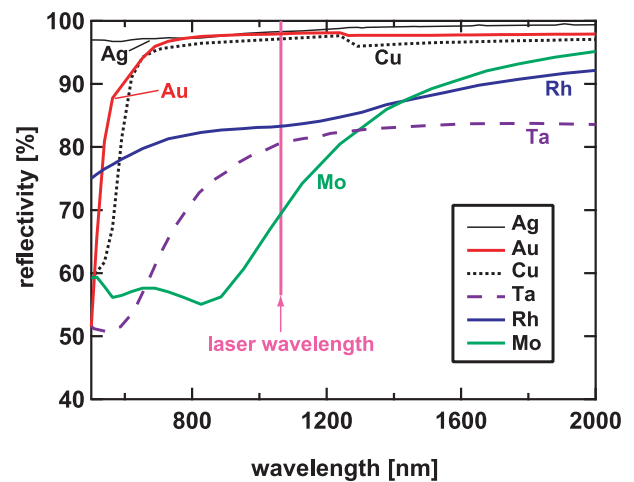


Fig. 2 Optical reflectivity as a function of wavelength for Ag, Au, Cu, Ta, Rh, and Mo [15].

Table 1 Melting point and reflectivity coefficient of temperature dependence [1] for the metals used in the calculation.

|      | Melting point [K] | coefficient $A$ [$K^{-1}$] |
|------|-------------------|----------------------------|
| Ag   | 1235.08           | $1.7 \times 10^{-5}$       |
| Au   | 1337.6            | $2.1 \times 10^{-5}$       |
| Cu   | 1357.6            | $3.0 \times 10^{-5}$       |
| Ta   | 3263              | $4.0 \times 10^{-5}$       |
| Rh   | 2233.15           | –                          |
| Mo   | 2894              | $7.0 \times 10^{-5}$       |

predict a reduction of 15% for the same increase in temperature [16].

We can evaluate the energy threshold for melting by calculating the surface temperature change in response to a laser pulse. When the pulse width is shortened, the effective pulse power increases, and additionally, the heat conduction length decreases. Therefore, the threshold pulse energy is a function of the pulse width; it increases with the pulse width. Figure 3 plots the LIDT as a function of the pulse width for (a) Ag, (b) Au, (c) Cu and Ta, and (d) Rh and Mo in the range of 50 ps - 50 ns. In Figs. 3 (a)-(d), the lines represent the calculated energy threshold for melting. The laser pulse shape was assumed to be a triangular, with rising and falling times equal to the pulse width. This assumption well approximates the Gaussian time dependence [17]. The dotted and solid lines represent the calculation results obtained using the calculated reflectivity and experimental reflectivity, respectively. In Fig. 3, the three types of experimentally deduced LIDT data, i.e., melting, slip deformation, and significant reflectivity change, summarized in Ref. [1] are also plotted. Here, significant reflectivity change corresponds to an indication of damage directly related to a change in reflectivity; it does not clearly differentiate between the reasons for the degradation in optical properties, such as "slip" or "melting." For example, Koumvakalis *et al.* [18] measured absorption by using a low-intensity laser reflected off the surface, and they determined a catastrophic damage pulse intensity beyond which the change in absorption is irreversible. On the other hand, Saito *et al.* [19] determined the damage threshold with using a scattering of a CW laser light and a dark field illumination technique. It is likely that the LIDT for slip deformation is in the range of one-half to one-fifth of that for melting. Plastic deformation due to pulsed laser-induced thermal stress followed by slip deformation has been considered to be a candidate mechanism for multiple-pulse damage to metal mirrors [20].

The threshold pulse energies for Ag and Au are almost same, as shown in Figs. 3 (a) and (b), respectively. In both cases, the solid line is about twice higher than the dotted line. The experimental melting threshold exists between the solid and dotted lines, indicating that the calculation is
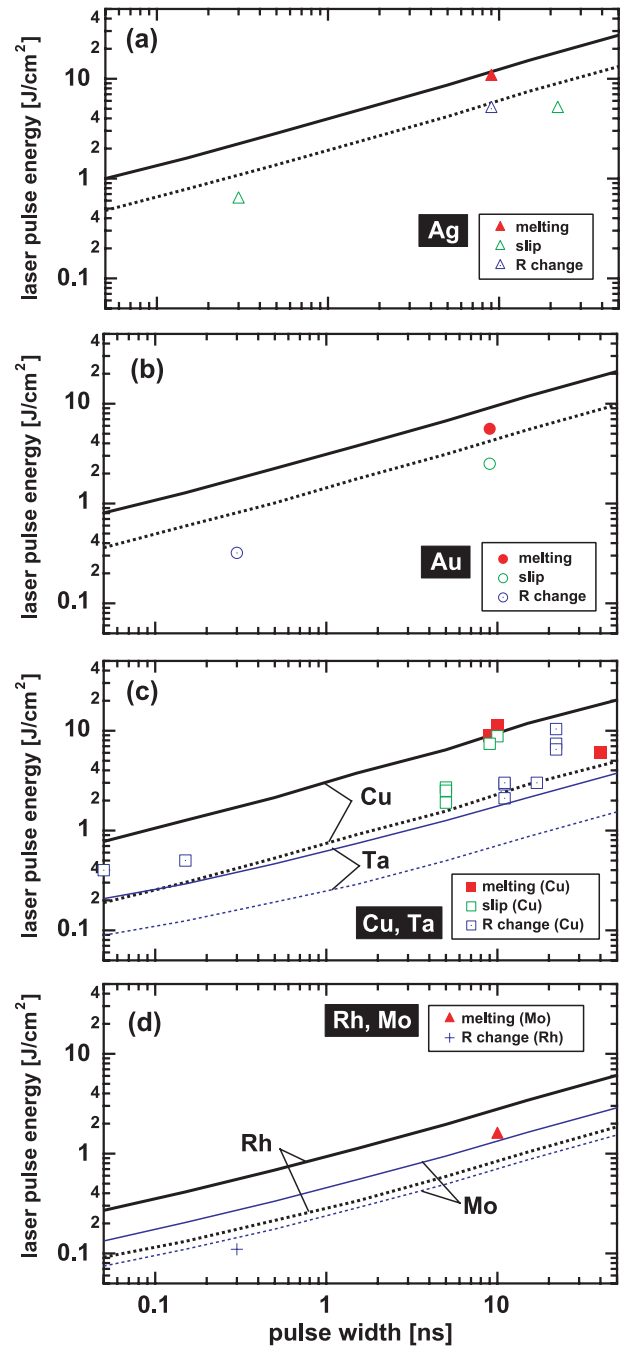


Fig. 3   Laser-induced damage threshold as a function of pulse width for (a) Ag, (b) Au, (c) Cu and Ta, and (d) Rh and Mo in the range of 50 ps - 50 ns. Dotted and solid lines represent the calculated melting threshold based on the calculated reflectivity and experimental reflectivity, respectively.

consistent with the experiments.

In the case of Cu, as shown in Fig. 3 (c), the range of scattering in experiments seems to be significant. Because the calculated degree of reduction in reflectivity with temperature for Cu is greater than that for Ag and Au, the difference between the solid and dotted lines becomes greater than those in Figs. 3 (a) and (b). The experimental results

have large ambiguity, as do the calculations; the experimental data are consistent with the solid line at 10 ns, while they are consistent with the the dotted line at 40 ns. Although the ambiguity in the temperature dependence of the reflectivity remains as an unknown factor, we can still use the calculation results as a benchmark for the assessment of the LIDT. In Fig. 3 (c), the calculations for Ta are additionally plotted. Even though the melting point of Ta is significantly high, as shown in Table 1, its threshold energy for melting is significantly lower than that for Cu because of its lower reflectivity and thermal conductivity.

Regarding Rh and Mo, as shown in Fig. 3 (d), we should say that their threshold energies are significantly lower than those of Au, Ag, and Cu, although their melting points are higher; their lower reflectivity cancels out the advantage. From Figs. 3 (a)-(d), we can say that the dotted lines, which represent the calculations based on the calculated reflectivity, afford the minimum melting thresholds in comparison with the solid line and the experimental melting threshold data. Thus, we use the calculation based on the calculated reflectivity as an indication of the LIDT.

Here, we should consider the effect of the number of pulses because the accumulation of slip deformation over multiple pulses can significantly decrease the LIDT. It has been observed that the LIDT decreases to approximately one-fifth for Cu and one-third for Mo when the pulse number increases to $2 \times 10^5$ [21]. For Ag, reductions to approximately half the original LIDT have been observed when the pulse number increases to $10^4$ [20]. It is suspected that the LIDT decreases to less than one-tenth of the one-pulse LIDT when the pulse number increases to $>10^8$ [21], the necessary pulse number for ITER diagnostics. Although the degree of reduction in the LIDT due to the multi-pulse effects varies by material, it is likely that the laser pulse energy should be reduced to at least 1/100 of the melting threshold when considering the multi-pulse effects and the fact that the threshold for the reflectivity change is one-half to one-fifth of the melting threshold. Based on this, in the next section, the discussion focuses on the specific characteristics required of the mirror for the ITER edge Thomson scattering diagnostics.

# 3. Mirror Design for ITER Edge Thomson Scattering System

Figure 4 shows a schematic illustration of the laser mirrors for the ITER edge Thomson scattering system. In the present design, two mirrors —a plane mirror and an off-axis parabolic mirror— are planned to be used for transmitting the laser beam to the vacuum chamber.

Figure 5 (a) shows the temporal evolution of the laser output energy used for the calculation. This temporal evolution is in fact that for the laser Thomson scattering used in JT-60U [22], which has a similar type of laser as that to be used for the ITER edge Thomson scattering system. Since two laser beams are combined to increase the laser
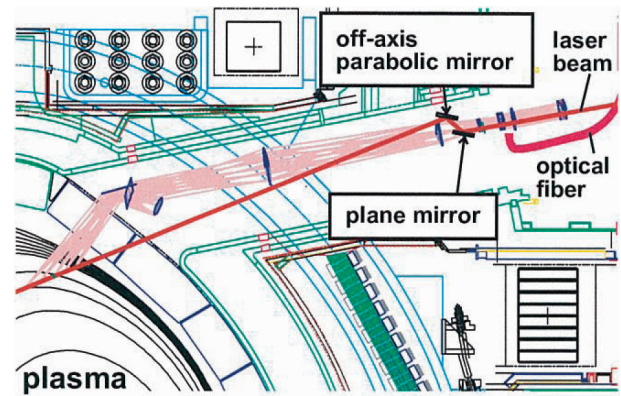


Fig. 4 Schematic illustration of collection optics and laser transmission system for the ITER edge Thomson scattering diagnostics. The arrangement of the plane mirror and off-axis parabolic mirror for laser transmission are presented.
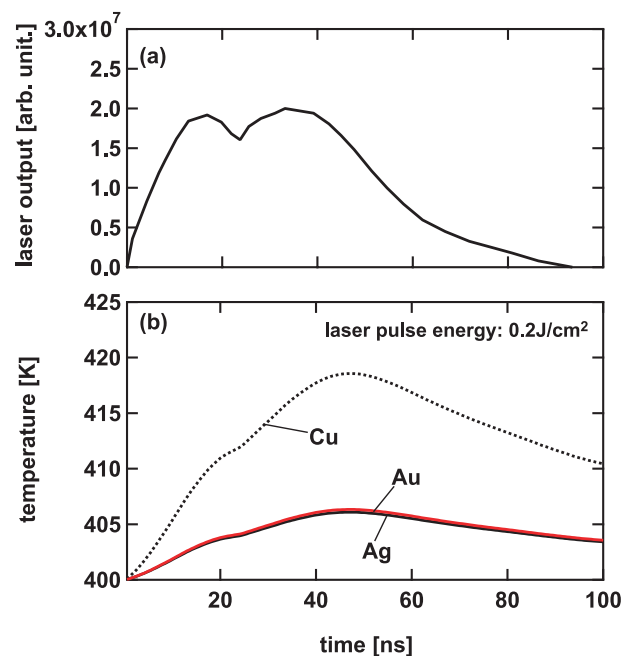


Fig. 5 (a) Temporal evolution of laser output used for the calculation. (b) Calculated temporal evolution of surface temperature for Au, Ag, and Cu at a pulse energy of 0.2 J/cm$^2$.

pulse energy for the laser system [23], the temporal evolution will have the double pulse shape shown in Fig. 5 (a). Figure 5 (b) shows the temporal evolution of the surface temperature for Au, Ag, and Cu in response to a laser pulse shown in Fig. 5 (a) with the pulse energy of 0.2 J/cm$^2$. Even though the laser output has double peaks, the surface temperature has only a single peak around ~50 ns.

Figure 6 shows the pulse energy dependences of the temperature increase for Au, Ag, Cu, Ta, Rh, and Mo until the melting temperature. The initial temperature before irradiation was assumed to be 400 K, which corresponds
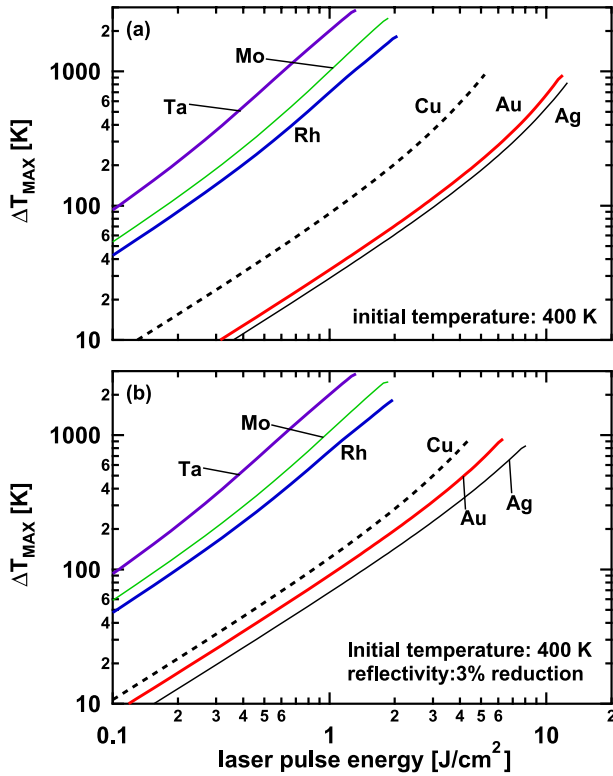
Fig. 6 Laser pulse energy dependences of the temperature increase for Ag, Au, Cu, Rh, and Mo under the condition that the surface temperature is less than the melting temperature. In (b), the calculations were performed with a 3% decrease in reflectivity.
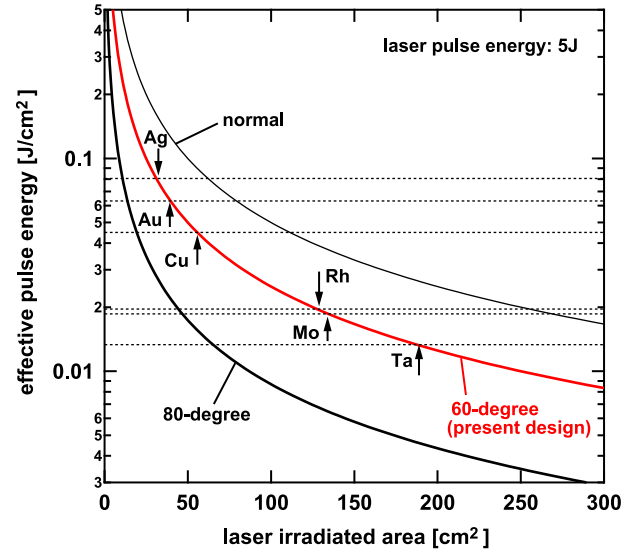


Fig. 7 Dependence of the effective pulse energy for different mirror materials on the laser size at different laser injection angles. One-hundredth of the calculated laser pulse energy for the melting threshold is plotted as an indication of the multi-pulse LIDT.

to the expected mirror temperature under the experiments. From the calculation, the threshold laser pulse energy increases with the reflectivity, as shown in Fig. 2; the threshold laser pulse energies for the metals are, respectively, 1.3, 1.9, 2.1, 5.2, 11.9, and 12.5 J/cm$^2$ for Ta, Mo, Rh, Cu, Ag, and Au. For diagnostic mirrors in fusion devices, there is concern that the reflectivity can be changed by the particle flux of neutrons and charge-exchange atoms and by contaminants, including the formation of metal and carbon films. If the reflectivity decreases with the flux, the deposited energy on the material increases, and consequently, the LIDT may decrease. It is planned that the mirror for the laser will be positioned far away from the plasma; thus, the significant reduction in reflectivity —by more than several tens of %— observed in the experiments with high-fluence irradiation [24, 25] should not occur. However, there remains concern that the reflectivity will change by several % during the course of multiple plasma shots. Figure 6 (b) shows the laser pulse energy dependences of the temperature increase for the different mirror materials assuming that the reflectivity has decreased by 3%. In Fig. 6 (b), the threshold laser pulse energies for the metals are decreased to 1.3, 1.9, 2.0, 4.5, 6.3, and 8.1 J/cm$^2$, respectively, for Ta, Mo, Rh, Cu, Ag, and Au. Concerning Rh, Mo, and Ta mirrors, the LIDT is almost same as that in the case without

degradation. In contrast, particularly for high-reflectivity metals (Ag, Au, and Cu), a slight reduction in reflectivity causes considerable decrease in the LIDT. This is attributed to the fact that the deposited heat on the material drastically increases with a slight reduction in reflectivity if the initial reflectivity is high, that is, if the initial deposited energy is low.

The laser pulse energy for the edge Thomson scattering system is expected to be 5 J. Since the wave incident on the final mirror will have $s$-polarization, the reflectivity will increase with the angle $\theta_{in}$, which is the angle between the normal vector of the mirror surface and the wave vector; and consequently, the LIDT will also increase with $\theta_{in}$ [26]. If the polarization was $p$-polarization, the reflectivity would decrease with the angle $\theta_{in}$. In order to take into account this angular dependence, we define the effective laser pulse energy at the mirror $I_{eff}$ as

$$I_{eff} = \cos(\theta_{in})I_{in}, \qquad (5)$$

where $I_{in}$ is the laser pulse energy at the surface in J/cm$^2$. That is, if the incident angle of the laser beam is $\theta_{in}$, the LIDT increases by a factor of $1/\cos(\theta_{in})$ from that for the normal direction case.

Figure 7 shows the dependence of the effective pulse energy on the laser irradiated area for different $\theta_{in}$, i.e., 0, 60, and 80°. The present design shown in Fig. 4 corresponds to the case of $\theta_{in} \sim 60°$. One hundredths of the calculated melting thresholds evaluated from Fig. 6 (b) are also plotted as dotted lines to indicate the multi-pulse LIDT. The intersection of the dotted line and the curve for 60° affords the necessary minimum mirror size. The necessary laser irradiated area decreases with the incident

Table 2 Minimum irradiated area on the mirror, minimum laser radius, and minimum mirror size for various metals evaluated from Fig. 7. The radial intensity profile of the laser beam is assumed to be flat.

|     | irradiated area ($cm^2$) | laser radius (cm) | mirror size (cm×cm) |
| --- | --- | --- | --- |
| Ag | 32 | 2.3 | $4.6 \times 9.1$ |
| Au | 40 | 2.6 | $5.1 \times 10.1$ |
| Cu | 56 | 3.0 | $6.0 \times 12.0$ |
| Ta | 189 | 5.5 | $11.0 \times 22.0$ |
| Rh | 129 | 4.6 | $9.1 \times 18.2$ |
| Mo | 134 | 4.7 | $9.3 \times 18.5$ |

angle, and less than half the area is necessary if $\theta_{in} = 80°$. Table 2 shows the minimum irradiated area on the mirror, minimum laser radius, and minimum mirror size evaluated from the results of Fig. 7. The radial intensity profile of the laser beam was assumed to be flat. Concerning Ag, for instance, the necessary mirror size is $4.6 \times 9.1$ cm, while that for Mo is four times larger. At present, the available space for the mirror is not well understood. However, some of the lenses in the collection optical system are larger than several hundreds of millimeters in diameter in the provisional design; the sizes in Table 2 are smaller. Thus, we should carefully investigate the mirror size by taking into account the available space and the minimum mirror size shown in Table 2.

Here, the necessary mirror size is estimated assuming that the spatial profile of the laser beam is uniform. A flat laser beam profile can be obtained using a serrated aperture with a pinhole, which has been successfully used in the JT-60 laser system [7]. In the laser system, the image-relaying optical system sustains the flat profile at the image point; however, the beam profile is distorted when the mirror is kept distant from the image point. Moreover, for a high-power solid-state laser, thermally induced optical distortion also produces a nonuniform profile accompanied by thermal lens effects, thermal birefringence, etc. [27]. Because the maximum laser power can be several times higher than that estimated as *(total power)/(beam area)*, it is better to choose a somewhat larger mirror than that listed in Table 2 by considering the nonuniformity of the laser beam profile.

For practical applications, we must also consider the feasibility of fabricating such a mirror. Regarding Cu, Ta, and Mo, it is likely that the mirror can be fabricated by polishing down bulk material. However, for Ta, there is concern because it absorbs gases such as deuterium and oxygen and becomes brittle. And in addition to this, because it has the worst characteristics in the calculation results, we do not recommend to use of Ta as the mirror material. Furthermore, it is suspected that fabrication of mirrors from bulk Au, Ag, or Rh may be difficult because of the high prices of Au and Rh and the softness of Au and Ag. Thus, it seems that only coating technique may be applicable for

fabricating such large-size mirrors for Au, Ag, and Rh. If coated mirrors are used, we must also consider the durability of the coating to multi-pulse effects. During the pulse, heat is conducted to more than $1 \mu m$ in depth; hence, it is necessary to consider the thickness of the coating layer and the bonding between the coating layer and the bulk material. The difference in LIDT between bulk and coated mirrors has been observed until now only in [28]; therefore, it is important to investigate further the durability of the coated material against multi-pulse effects. Although Ag has best reflectivity among the candidate materials, the disadvantage is that it is easily eroded by oxidant and chlorine, leading to decreased reflectivity. Thus, it is likely that the use of improved Ag-based alloy [29, 30] would be a better solution. On the other hand, Cu is both cheaper and harder than Au and Ag, and is therefore also a plausible material. And since oxygen-free Cu is not very hard, diamond turning could be used to fabricate the Cu mirror. It is likely that Cu mirrors may be fabricated mechanically by improving the hardness with the addition of small amount of other materials, typically less than several %, such as chromium, cobalt, and beryllium [31].

At this point, we should say that the nuclear transmutation effects on the material have not been discussed in the present paper. For example, Au changes to mercury [32] and Mo to niobium [33] by nuclear transmutation. The vaporization of this mercury may roughen the mirror surface, while niobium has similar reflectivity to that of Mo at 1064 nm. By considering these effects, the rank or order of preference of metals for the fabrication of the in-vessel mirror may change. Therefore, in future studies, it will be necessary to quantitatively investigate the effects of nuclear transmutation and to then decide on the appropriate material by also considering the feasibility of fabrication.

Although only metal mirrors have been considered in the present paper, it would also be attractive if dielectric multi-layer coated mirrors could be used for the in-vessel laser transmission mirrors because they have reflectivity greater than 99 %. In [34], a multi-layer coated mirror was exposed to radiation, but the reduction in the reflectivity was not observed. Only a few studies have been reported in relation to the effects of radiation on multi-layer coated

mirrors; thus, further experimental investigation is necessary to confirm the durability of multi-layer coated mirrors.

# 4. Conclusions

The optimum metals for laser mirrors were discussed based on the numerical analysis. A comparison between the calculation results and current laser-induced damage threshold (LIDT) data was presented. They were found to be consistent with each other in the range of experimental ambiguity and the ambiguity in the temperature dependence of optical reflectivity. From the perspective of the low LIDT due to the high reflectivity, silver, gold, and copper remain plausible materials. Gold and silver seem to be good choices because of their high reflectivity and LIDT. However, there remains concern about the feasibility fabricating mirrors from silver and gold, which may be too soft for polishing. On the other hand, copper is both cheaper and harder than gold and silver, and is therefore also a plausible candidate material. The necessary minimum mirror size for a copper mirror is estimated to be $6\,\mathrm{cm} \times 12\,\mathrm{cm}$ for the ITER edge Thomson scattering system. As future work, detailed experimental investigations concerning multi-pulse effects by considering the degradation in reflectivity due to the exposure to neutral particles and radiation (neutron and gamma ray) are important.

# Acknowledgments

[1] V.S. Voitsenya, V.G. Konovalov, M.F. Becker, O. Motojima, K. Narihara and B. Schunke, Rev. Sci. Instrum. **70**, 2016 (1999).
[2] V. Voitsenya, A. Bardamid, V. Bondarenko, W. Jacob, V. Konovalov, S. Masuzaki, O. Motojima, D. Orlinskij, V. Poperenko, I. Ryzhkov, A. Sagara, A. Shtan, S. Solodovchenko and M. Vinnichenko, J. Nucl. Mater. **290-293**, 336 (2001).
[3] D.V. Orlinski, V.S. Voitsenya and K.Y. Vukolov, Plasma Devices and Operations **15**, 33 (2007).
[4] R.M. Wood, *Laser Damage in Optical Materials* (IOP Publishing, 1986).
[5] *Design Description Document (DDD) ITER diagnostic system, (WBS5.5), July, 2000* (2000).
[6] T. Hatae, H. Kubomura, S. Matsuoka and Y. Kusama, JAEA-Technology **2006-021**, (2006).
[7] T. Hatae, O. Naito, M. Nakatsuka and H. Yoshida, Rev. Sci. Instrum. **77**, 10E508 (2006).
[8] S. Kajita, D. Nishijima, N. Ohno and S. Takamura, J. Appl. Phys. **100**, 103304 (2006).
[9] Japan Society of Thermophysical Properties, *Thermophysical Property Handbook* (Yokendo, Tokyo, 2000).
[10] *Thermophysical properties of high temperature solid materials* (Macmillan, New York, 1967).
[11] P. Paradis, T. Ishikawa and S. Yoda, Int. J. Thermophysics **24**, 1121 (2003).
[12] T. Aisaka and M. Shimizu, Nucl. Instrum. Methods **28**, 646 (1970).
[13] S.C. Jain, B.B. Sharma and B.K. Reddy, J. Phys. D: Appl. Phys. **5**, 155 (1972).
[14] A.G. Sorokin, L.N. Trukhanova and L.P. Filippov, High Temperature **7**, 342 (1969).
[15] E.D. Palik (Editor), *Handbook of Optical Constants of Solids* (Academic Press, Orlando, 1985).
[16] K. Ujihara, J. Appl. Phys. **43**, 2376 (1972).
[17] J. Lin and T.F. George, J. Appl. Phys. **54**, 382 (1983).
[18] N. Koumvakalis, C. Lee and M. Bass, IEEE J. Quantum. Electron. **QE-19**, 1482 (1983).
[19] T. Saito, D. Milam, P. Baker and G. Murphy, National Bureau of Standards Special Publication **N435**, 29 (1975).
[20] C.S. Lee, N. Koumvakalis and M. Bass, J. Appl. Phys. **54**, 5727 (1983).
[21] D.V. Orlinski, V.S. Voitsenya and K.Y. Vukolov, Plasma Devices and Operations **15**, 127 (2007).
[22] T. Hatae, M. Nakatsuka and H. Yoshida, J. Plasma Fusion Res. **80**, 870 (2004).
[23] H. Yoshida, M. Nakatsuka, T. Hatae, S. Kitamura and T. Kashiwabara, Jpn. J. Appl. Phys. **42**, 439 (2003).
[24] M. Ye, S. Fukuta, N. Ohno, S. Takamura, K. Tokunaga and N. Yoshida, J. Plasma Fusion Res. SERIES **3**, 265 (2000).
[25] T. Sugie, S. Kasai, M. Taniguchi, M. Nagatsu and T. Nishitani, J. Nucl. Mater. **329-333**, 1481 (2004).
[26] J.F. Figueira and S.J. Thomas, IEEE J. Quantum. Electron. **QE-18**, 1381 (1982).
[27] W. Koechner, *Solid-state laser engineering*, 5th ed. (Springer, 1999).
[28] A. Gorshkov, I. Bel'bas, M. Maslov, V. Sannikov and K. Vukolov, Fusion Eng. Des. **74**, 859 (2005).
[29] J. Nakai, T. Yuki, H. Fujii, T. Satou, T. Onishi and K. Takagi, Kobe Steel Engineering Report **52**, 12 (2002).
[30] T. Higuchi and H. Koyanagi, Jpn. J. Appl. Phys. **39**, 933 (2000).
[31] E.A. Brandes and G.B. Brook, *Smithells Metals Reference Book*, 7th ed. (Butterworth-Heinemann, 1998).
[32] T. Nishitani, T. Shikama, R. Reichle, E.R. Hodgson, E. Ishitsuka, S. Kasai and S. Yamamoto, Fusion Eng. Des. **64-64**, 437 (2002).
[33] A. Kumar, Y. Ikeda and M. Abdou, J. Nucl. Mater. **240**, 144 (1997).
[34] I. Orlovskiy and K. Vukolov, Fusion Eng. Des. **74**, 865 (2005).